

Calculation of Streaklines for Time Periodic Flows

Moshe Rosenfeld*

Tel-Aviv University, Tel-Aviv 69978, Israel

The calculation of streaklines for complex time-dependent flows is confronted with severe difficulties due to the huge data sets involved. In the present work we propose a storage reduction method for time-periodic flows. The method is based on the observation that many time-periodic flows can be accurately approximated using a small number of Fourier terms. By storing only the significant harmonics of the Fourier decomposition, the storage (disk space and core memory) required for calculating streaklines can be reduced by one order of magnitude or more. The reduced storage permits the calculation of the streaklines after completing the solution of the equations, rather than calculating a set of predefined streaklines simultaneously with the solution of the flow. This significantly enhances the capability of studying interactively complex flowfields. Test cases confirm the assumption that a small number of Fourier terms is adequate for calculating accurately the streaklines of complex flows.

Introduction

THE simulation of time-dependent flows is one of the major topics of interest in contemporary computational fluid dynamics (CFD) studies. With the increase in computing power availability, complex unsteady flows can be calculated, creating huge data sets. In typical three-dimensional cases, $\mathcal{O}(10^6)$ mesh points and $\mathcal{O}(10^4)$ time steps are required, generating data sets of $\mathcal{O}(10^{10})$ words of storage. In two-dimensional cases less storage is required [$\mathcal{O}(10^8)$ words], but still it might be excessive even when large supercomputers are used, not to mention workstations that are mostly used for postprocessing the results.

These large data sets confront difficult challenges in the postprocessing of flow simulations. One of the common flow visualization techniques is based on the calculation of the streaklines that mimic dye-injection experiments. This calculation is computationally intensive. Yet, the main obstacle in the case of time-dependent flows is the need to store (both on disk and in memory) large data sets (the whole evolution of the flow). One way to overcome this problem is to calculate the streaklines simultaneously with the solution of the flow equations. This necessarily means that the release points and release rate of the particles should be predetermined. The flow cannot be studied interactively, which is a severe shortcoming in the case of complex flowfields.

Time-periodic flows are a special class of time-dependent flows. Time-periodic flows are obtained as self-excited flows (e.g., the von Kármán vortex street) or by forced oscillating perturbations (e.g., the flow in blood vessels or certain hydraulic devices). Simple time-periodic flows (with a narrow spectra) are mostly found in low or intermediate Reynolds (Re) number cases, but certain high Reynolds number flows can be also approximated as periodic flows.

In the present article, we suggest how to overcome some of the problems associated with the calculation of streaklines in time-periodic flows by using the Fourier transform of the solution. The solution itself is obtained from any unsteady flow solver. This approach might be appealing if a small number of harmonics can accurately approximate the time-dependent solution. We will demonstrate that in certain cases the saving in storage space and core memory might be more than one order of magnitude. This saving can be utilized for calculating streaklines interactively even for solutions employing a very large number of mesh points, a task that is in many cases impossible otherwise.

Methodology

To take advantage of the time periodicity of the flow in the calculation of the streaklines, an existing solution of the Cartesian velocity components $\mathbf{u} = (u, v, w)$ is decomposed into a Fourier series

$$\mathbf{u}(\mathbf{x}, t) = \sum_{n=0}^M \mathbf{A}_n(\mathbf{x}) \cos \left[2\pi n \frac{t}{T} - \varphi_n(\mathbf{x}) \right] \quad (1)$$

where the Cartesian coordinates are $\mathbf{x} = (x, y, z)$, \mathbf{A}_n , and φ_n are the amplitude and phase angle of the harmonic n , T is the fundamental period, and N is the maximal discrete harmonic number. The main assumption of the present study is that the Fourier series converges fast for certain time-periodic flows and, therefore, a small number of harmonics can approximate the solution accurately. Thus, in the present approach the governing equations are advanced in time by any available time-dependent flow solver until a time-periodic solution is obtained (assuming it exists). The velocity field is saved for a single cycle and then transformed into a Fourier series. Only the N_{\max} significant harmonics ($N_{\max} \leq M$) are stored for future processing. The success of the storage reduction method depends on the number of significant harmonics required to restore accurately the velocity field. In the Results section N_{\max} is determined for two typical cases.

The path of a particle is computed by a standard second-order Runge-Kutta scheme,

$$\begin{aligned} \mathbf{x}^* &= \mathbf{x}^n + \mathbf{u}(\mathbf{x}^n, t^n) \Delta t \\ \mathbf{x}^{n+1} &= \mathbf{x}^n + \frac{1}{2} [\mathbf{u}(\mathbf{x}^*, t^{n+1}) + \mathbf{u}(\mathbf{x}^n, t^n)] \Delta t \end{aligned} \quad (2)$$

where n and $n+1$ are the old and new time levels, respectively, t is the time, and the time step is $\Delta t = t^{n+1} - t^n$. The varying time-step size is determined from the requirement that the maximal distance the particle passes in Δt does not exceed 0.2 of the local cell size, according to common practices. To generate the streaklines, particles are released at a constant rate from several points in the flowfield, and the locations of all of the particles are plotted for certain phases of the cycle.

The difference between existing streakline calculation methods, which will be referred to as the standard methods, and the present method lies in the source of the velocity vector \mathbf{u} . In the standard method \mathbf{u} is stored in the physical domain, whereas in the present method it is computed as needed from the inverse Fourier transform. Using the standard method, the computation of $\mathbf{u}(\mathbf{x}, t^n)$ requires interpolation both in time and space. In the present method, however, only spatial interpolation is required because the inverse Fourier transform can be calculated for any time. The Fourier decomposition is used as a high-accuracy interpolating tool in time.

Received Sept. 20, 1994; revision received Feb. 24, 1995; accepted for publication March 22, 1995. Copyright © 1995 by the American Institute of Aeronautics and Astronautics, Inc. All rights reserved.

*Lecturer, Department of Fluid Mechanics and Heat Transfer, Faculty of Engineering, Member AIAA.

Results

The proposed method for calculating the streaklines is tested for two-dimensional time-periodic flows. The first test case considers the self-excited vortex shedding behind a circular cylinder, and the second case considers the internal forced pulsating flow in a constricted channel. These two cases represent a wide range of external and internal time-periodic flows. In each case, the validity of the assumption that the Fourier series converges fast is examined. It will be shown that, indeed, a small number of harmonics can accurately represent the streaklines, thus significantly reducing the storage requirements and, in some cases, even the CPU time.

In the present study, the laminar unsteady incompressible Navier-Stokes equations with primitivelike variables are solved with a solution procedure developed by Rosenfeld et al.¹ and Rosenfeld and Kwak.^{2,3} The governing equations written in integral form are discretized by finite volumes. The scheme is second-order accurate in space and time. The discrete equations are solved by a fractional step method with an approximate factorization of the momentum equations. The convergence rate of the Poisson equation is accelerated by a multigrid procedure. The interested reader may find the details in the references cited, where the method was also validated for a series of internal and external flow problems.

Circular Cylinder Case

A very popular test case of numerical solutions of time-dependent viscous flows is the circular cylinder at a Reynolds number of 200; for example, see Refs. 1 and 4. It represents many laminar self-excited external flows over bluff bodies. The outer circular boundary is at a distance of 30.5 from the center of the circular cylinder (all distances and coordinates of the present test case are nondimensionalized by the diameter of the cylinder). A mesh of 513×513 points was generated with clustering of grid points near the circular cylinder, the upstream stagnation point, and in the wake region. It was shown⁴ that a grid-independent solution was obtained for that mesh. Additional numerical and other details can be found in Ref. 4.

The spectra of the velocity components are given in Fig. 1 for two representative points. Point A is in the formation region of the vortices ($x = 0.9$ and $y = 0.4$ in a coordinate system with the origin at the center of the cylinder), whereas point B is in the propagation region of the vortices ($x = 7$ and $y = 0.4$). A decrease of more than two orders of magnitude is obtained for $n \geq 4$, supporting the assumption that a small number of harmonics can approximate the solution accurately.

To calculate the streaklines, 600 particles per cycle were released from 24 points along the upstream and downstream symmetry lines. The paths of all of the particles were calculated by integrating Eq. (2) until the particles left the domain of solution. The locations of the particles are shown in Fig. 2 for the instant when the lift coefficient is zero. The streaklines were calculated using the standard method (labeled as exact), as well as by the present method with an increasing number of harmonics (N_{\max}) included in the inverse Fourier transformation.

The main features of the flow (the shedding of the vortices and the downstream propagating street of vortices) are obtained even if only the mean and the first harmonic are used to reconstruct the velocity field in the physical domain ($N_{\max} = 1$). Yet, the size and shape of the vortices are different from that obtained from the exact

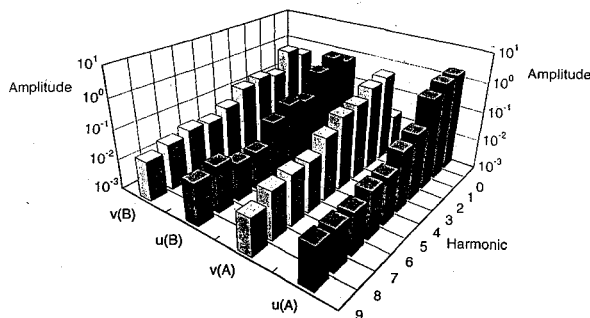


Fig. 1 Spectra of the velocity components, circular cylinder.

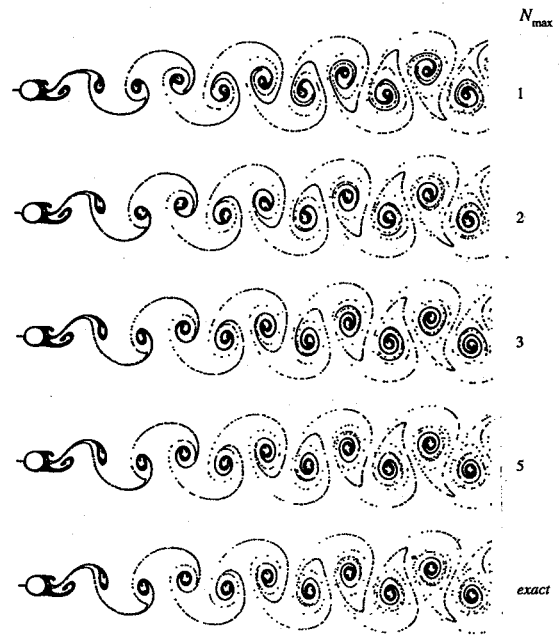


Fig. 2 Dependence of the streaklines on the number of harmonics, circular cylinder.

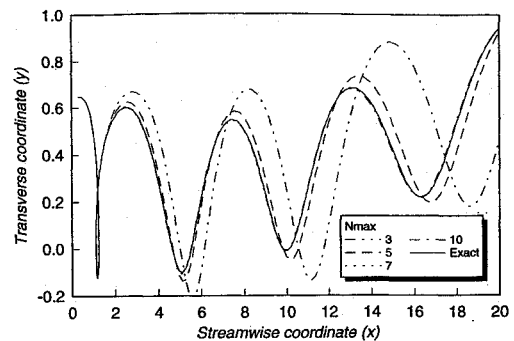


Fig. 3 Dependence of a particle trace on the number of harmonics, circular cylinder.

solution, although the spacing between the vortices (the wavelength) is identical. Adding the second harmonic ($N_{\max} = 2$) improves the agreement with the exact solution. The streaklines computed using at least three harmonics are visually indistinguishable from the streaklines calculated by the standard method.

The effect of N_{\max} was quantitatively studied in Fig. 3 by comparing the trace of a single particle released from the point (0.3, 0.6) at the start of the cycle. Good agreement is obtained even for $N_{\max} = 5$ as long as $x < 8$. For longer integration time, more harmonics are needed to preserve the accuracy because of the accumulation of errors. The location of the particle at the most downstream point shown in Fig. 3 ($x = 20$) for the case of $N_{\max} = 7$ is within a distance of less than 0.005 diameters from that calculated by the standard method.

Figure 2 presents the streaklines of a large set of points and revealed a better overall similarity with the standard calculation for lower N_{\max} than the individual particle trace of Fig. 3. It might be a result of an averaging phenomenon that occurs if a large number of particles are plotted simultaneously. The average accumulated integration errors of many particles seem to cancel out, giving a more favorable agreement for smaller N_{\max} than each of the individual particles.

Constricted Channel Case

The geometry of the computational domain of the constricted channel case is sketched in Fig. 4. The channel is composed of two straight parallel plates placed at a distance h apart (all of the length units of this case are scaled by h). On the upper wall, a

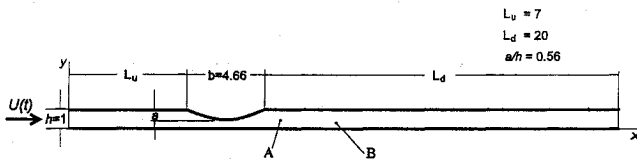


Fig. 4 Geometry of the constricted channel case (not to scale).

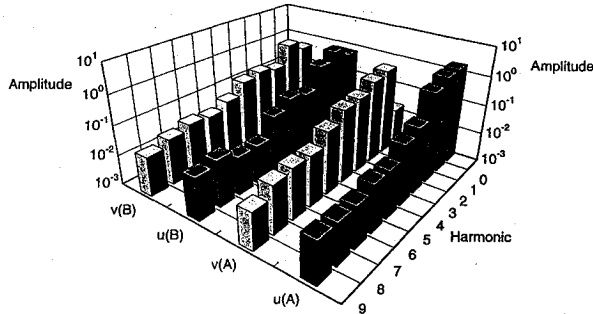


Fig. 5 Spectra of the velocity components, constricted channel.

circular-arc constriction is added with a size of $a/h = 0.56$. A mesh with 97×417 points in the transverse and axial directions, respectively, is employed. A pulsating flow is forced at the upstream boundary. The waveform of the incoming average axial velocity $U(t)$ consists of a steady flow in the first-half of the cycle, $U(t) = U_s$, followed by a half-sinus superimposed on the steady component in remainder of the cycle, $U(t) = U_s - U_p \sin(2\pi t/T)$. The period is T , and $U_s = 1$, and $U_p = 1.2$. The Reynolds and Strouhal numbers (based on the mean incoming velocity) are $Re = 720$ and $St = 0.368$.

The geometry, the incoming waveform, and the Strouhal number were chosen to be identical to one of the cases considered in the experiments of Park.⁵ The reason is that detailed comparisons of the numerical results with these experimental results were carried out by Rosenfeld.⁶ The vortical flowfield was accurately captured by the numerical simulations, and very good agreement was obtained in the propagation speed of the vortices for a wide range of parameters. In addition, the numerical model and the calculated results were extensively tested for numerical consistency and accuracy.⁶ It was shown that the mesh size and the number of time steps were adequate and that the location and type of boundary conditions were correctly chosen.

The characteristics of the flowfield were described by Rosenfeld⁶ and, therefore, it will be only very briefly mentioned here. A new pair of vortices is developed in each cycle leewards of the constriction, one vortex near each wall. At every instant, vortices generated in previous cycles still coexist downstream, creating two trains of downstream moving vortices near the walls and a wavy core flow between them.

The spectra of the velocity components are given in Fig. 5 for two representative points. The approximate locations of the points are shown in Fig. 4. Similar to the circular cylinder case, point A is in the formation region of the lower wall vortex ($x = 12.5$, $y = 0.3$ in a coordinate system with the origin at the upstream part of the lower wall; the downstream edge of the constriction is at $x = 11.7$) whereas point B is in the propagation region (14.5 , 0.2). In the present internal flow case, the higher harmonics are more significant than in the circular cylinder case. Nonetheless, a decrease of two orders of magnitude is still obtained for $N_{\max} > 10$. The effect of the Reynolds number was studied by solving the same case for $1440 > Re > 90$. The spectra and the convergence rate with the harmonic number showed insensitivity to Reynolds number in the range tested. This further supports the assumption that a small number of harmonics can, indeed, approximate the solution accurately, even for relatively high-laminar Reynolds numbers.

In the present case, the streaklines were computed as a function of N_{\max} , in addition to the standard (exact) method. Figure 6 shows the streaklines downstream of the constriction for $t/T = 0.4$. Particles were released at a rate of 500 per cycle from nine points in the throat

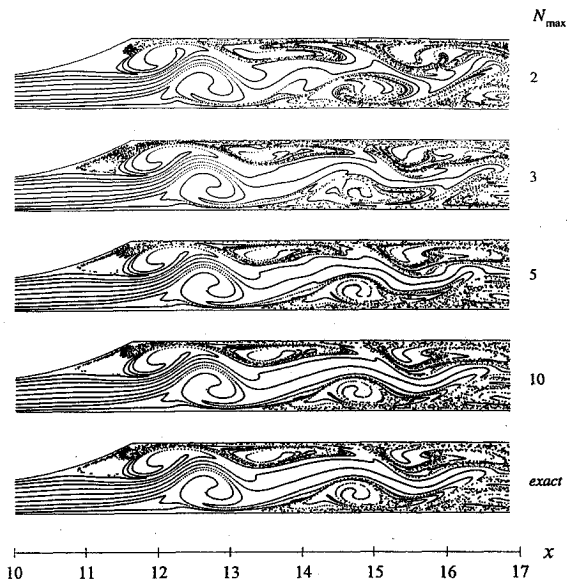


Fig. 6 Dependence of the streaklines on the number of harmonics, constricted channel.

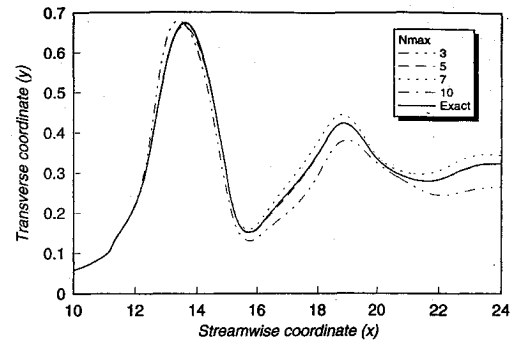


Fig. 7 Dependence of a particle trace on the number of harmonics, constricted channel.

of the constriction. Even a small number of harmonics ($N_{\max} = 2$) can capture the global flow structures, however, significant differences exist in the smaller scale structures. The differences with the exact streaklines diminish as more harmonics are added to the inverse Fourier transformation. The streaklines obtained for $N_{\max} = 10$ are graphically identical to those obtained from the standard method.

The effect of N_{\max} was quantitatively studied in Fig. 7 by comparing the trace of a single particle released from $x = 9.5$, $y = 0.05$ at the start of the cycle. Good agreement is obtained, even for $N_{\max} < 7$ for an integration that does not exceed $x = 17$. For longer integration, more harmonics are needed to preserve the accuracy; $N_{\max} = 10$ results in a graphically identical particle trace to the exact (standard) solution.

Discussion

The main motivation for using the Fourier decomposition of the velocity field is the possible saving in disk storage and core memory in the calculation of the streaklines (the same techniques can be used for other purposes as well⁷). The two flow cases considered in the present work might give indications of the possible gains for relatively low Reynolds number laminar flows. In the circular cylinder case, 800 time steps per cycle were computed but only every eighth step was stored (because we could not afford more storage and core memory). Thus, 100 time steps were used for the calculation of the streaklines in the standard method. The results described in the preceding section show that seven harmonics are sufficient to calculate the streaklines accurately. The required storage is equivalent to $1 + 7 \times 2 = 15$ time steps (for the mean and the amplitude and phase angle of each harmonic), i.e., the saving is by a factor of almost 7. In the constricted channel case, that represents a more complex flowfield, 10 harmonics are needed to restore the solution

Table 1 Comparison of the memory requirements for the two test cases

	Mesh	Standard method		Present method	
		N_T	Memory, Mbytes	N_{max}	Memory, Mbytes
Circular cylinder	263,169	100	201	7	30
Constricted channel	40,643	100	31	10	6.5

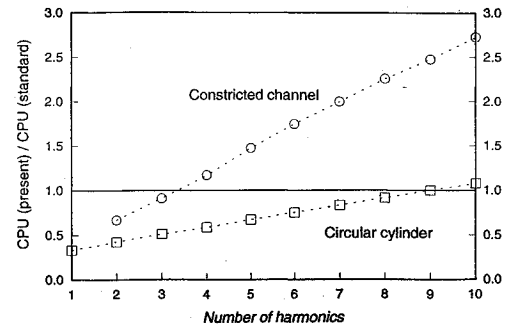
accurately, and the required storage is equivalent to 21 time steps. In this case 100 time steps were stored as well, although 200 time steps per cycle were computed. The saving reduces by a factor of 5, which is still very significant in terms of the required memory as Table 1 reveals. In Table 1, the required memory refers to the core memory (and disk space) in megabytes required for the two velocity components using single precision words; N_T is the number of time levels stored per cycle.

The reduction in the memory offered by the present method might be the only possibility to calculate the streaklines interactively. For example, in the circular cylinder case a minimum of 201 Mbytes of memory are required for the standard method, Table 1. In many cases, especially if workstations are used for postprocessing of the results, this amount of memory is unavailable. Similar savings are anticipated for three-dimensional flows as well. But since in these cases the storage required for each time step is at least one order of magnitude larger, the storage reduction offered by the present method is crucial. Without this saving, the streaklines cannot be computed interactively because of excessive core memory requirements. Of course, virtual memory can be used in these cases, but then the computations are very inefficient.

The number of harmonics needed to be stored is problem dependent and general guides cannot be offered. The analyst has to critically test the validity of the method for each class of calculations. The experience with the two test cases, however, as well as with additional (undocumented) studies, show that for many low and medium Reynolds number laminar flows ($Re < 2000$, problem dependent), 10–20 harmonics are more than adequate. The method might work equally well for turbulent flow simulations as well, as long as turbulence is modeled rather than directly simulated (in the former case, the spectra of the velocity is narrow since only the mean flow is calculated). Moreover, there are many indications that an even smaller number of harmonics can predict reasonably well the global features of the flow. The number of harmonics depends also on the length of integration because of the accumulation of errors (Figs. 3 and 7). If only a short-time integration of Eq. (2) is required, fewer harmonics can be used. It should be noted that the reconstruction of primitive flow variables per se demands less harmonics than that required for the calculation of the streaklines. Thus, if streaklines are not required, an even larger saving in storage can be obtained.⁷

The CPU time needed for performing the calculation of the streaklines is another parameter that should be compared when assessing the methods. The reconstruction of the velocity field from the Fourier components requires additional computations. The more harmonics, the higher the penalty in CPU time. On the other hand, the smaller memory required by the present method may accelerate the calculations because no swapping to disk is necessary and more cache hits are achieved.

Figure 8 plots the relative CPU time needed to compute the streaklines of the constricted channel case (Fig. 5) as a function of the

**Fig. 8 Dependence of the relative CPU time on the number of harmonics.**

number of harmonics (N_{max}) included in the inverse Fourier transformation. The relative CPU time is the CPU time relative to the standard method. All of the calculations were carried out on a DEC 3000/400 Alpha workstation with 128 Mbyte RAM memory. Up to three harmonics, the present method requires less CPU time than the standard method. Adding more harmonics, however (as is required in most cases), increases the CPU time. The CPU time requirement might significantly change in favor of the present method if disk swapping is necessary because of the large data sets involved in the standard method. The circular cylinder represents such a case (Table 1). The relative CPU time for this case, also shown in Fig. 8, reveals that for $N_{max} < 10$ the present method requires less CPU time than the standard method. Thus, when a large number of mesh points are used (such as in three-dimensional cases), the present method might require not only reduced memory but also less CPU time.

The overhead of the present method in terms of CPU time originates from the necessity to perform inverse Fourier transforms. These operations can be greatly benefited by taking advantage of special software/hardware capabilities of existing workstations and digital signal processor (DSP) cards to perform such operations efficiently. This requires more sophisticated programming techniques, but the anticipated acceleration may well pay off.

References

- Rosenfeld, M., Kwak, D., and Vinokur, M., "A Fractional-Step Solution Method for the Unsteady Incompressible Navier-Stokes Equations in Generalized Coordinate Systems," *Journal of Computational Physics*, Vol. 94, No. 1, 1991, pp. 102–137.
- Rosenfeld, M., and Kwak, D., "Time-Dependent Solutions of Viscous Incompressible Flows in Moving Coordinates," *International Journal for Numerical Methods in Fluids*, Vol. 13, No. 10, 1991, pp. 1311–1328.
- Rosenfeld, M., and Kwak, D., "Multi-Grid Acceleration of Fractional Step Solvers of Incompressible Navier-Stokes Equations in Generalized Curvilinear Coordinate Systems," *AIAA Journal*, Vol. 31, No. 10, 1993, pp. 1792–1800.
- Rosenfeld, M., "Grid Refinement Test of Time-Periodic Flows over Bluff Bodies," *Computers and Fluids Journal*, Vol. 23, No. 5, 1994, pp. 693–709.
- Park, D. K., "A Biofluid Mechanics Study of Arterial Stenoses," M.S. Thesis, Dept. of Mechanical Engineering, Lehigh Univ., Bethlehem, PA, May 1989.
- Rosenfeld, M., "Validation of Numerical Simulation of Incompressible Pulsatile Flow in a Constricted Channel," *Computers and Fluids Journal*, Vol. 22, No. 2/3, 1993, pp. 139–156.
- Rosenfeld, M., "Utilization of Fourier Decomposition for Analyzing Time-Periodic Flows," *Computers and Fluids Journal*, Vol. 22, No. 4, 1995, pp. 349–368.